European Heart Journal (2010) **31**, 2301–2309
doi:10.1093/eurheartj/ehq107

SIRT1 decreases Lox-1-mediated foam cell formation in atherogenesis

Sokrates Stein[1,2], Christine Lohmann[1,2], Nicola Schäfer[1,2], Janin Hofmann[3], Lucia Rohrer[2,4], Christian Besler[1,2], Karin M. Rothgiesser[5], Burkhard Becher[2,3], Michael O. Hottiger[2,5], Jan Borén[6], Michael W. McBurney[7], Ulf Landmesser[1,2], Thomas F. Lüscher[1,2], and Christian M. Matter[1,2]*

[1]Cardiovascular Research, Institute of Physiology, Zurich University and Cardiology, Cardiovascular Center, University Hospital Zurich, Winterthurerstrasse 190, CH-8057 Zurich, Switzerland; [2]Zurich Center for Integrative Human Physiology (ZIHP), Zurich CH-8057, Switzerland; [3]Neuroimmunology Unit, Inst. Experimental Immunology, Zurich CH-8057, Switzerland; [4]Institute for Clinical Chemistry, Zurich CH-8057, Switzerland; [5]Institute of Veterinary Biochemistry and Molecular Biology, University of Zurich and University Hospital Zurich, Zurich CH-8057, Switzerland; [6]Sahlgrenska Center for Cardiovascular and Metabolic Research, University of Goteborg, Goteborg SE-41345, Sweden; and [7]Department of Medicine, Ottawa Health Research Institute, University of Ottawa, Ottawa, ON, Canada K1Y 4E9

Received 11 October 2009; revised 26 February 2010; accepted 12 March 2010; online publish-ahead-of-print 23 April 2010

This paper was guest edited by Prof. Stefan Janssens, University Hospital Gasthuisberg, Leuven, Belgium

Aims Endothelial activation, macrophage infiltration, and foam cell formation are pivotal steps in atherogenesis. Our aim in this study was to analyse the role of SIRT1, a class III deacetylase with important metabolic functions, in plaque macrophages and atherogenesis.

Methods and results Using partial *SIRT1* deletion in atherosclerotic mice, we demonstrate that SIRT1 protects against atherosclerosis by reducing macrophage foam cell formation. Peritoneal macrophages from heterozygous *SIRT1* mice accumulate more oxidized low-density lipoprotein (oxLDL), thereby promoting foam cell formation. Bone marrow-restricted *SIRT1* deletion confirmed that SIRT1 function in macrophages is sufficient to decrease atherogenesis. Moreover, we show that SIRT1 reduces the uptake of oxLDL by diminishing the expression of *lectin-like oxLDL receptor-1* (*Lox-1*) via suppression of the NF-κB signalling pathway.

Conclusion Our findings demonstrate protective effects of SIRT1 in atherogenesis and suggest pharmacological SIRT1 activation as a novel anti-atherosclerotic strategy by reducing macrophage foam cell formation.

Keywords SIRT1 • Macrophage foam cell • Atherogenesis

Introduction

Atherosclerosis is a chronic inflammatory disease that results from interaction between oxidized low-density lipoprotein (oxLDL), activated endothelial cells, monocyte-derived macrophages, T cells, and the arterial wall. Activated endothelial cells express adhesion molecules, e.g. vascular cell adhesion molecule 1 (VCAM-1) and intercellular adhesion molecule-1 (ICAM-1), which attract and recruit blood monocytes to the vessel wall. These monocytes differentiate into macrophages and infiltrate to the sub-endothelial space where they release and respond to inflammatory mediators such as tumour necrosis factor-α (TNFα), VCAM-1, and interleukins (IL). Eventually, these inflammatory macrophages ingest oxLDL via scavenger receptors, such as scavenger receptor-A (SR-A), CD36 or lectin-like oxLDL receptor 1 (Lox-1), becoming foam cells, and thereby promoting plaque formation.[1]

Sir2 is an NAD-dependent class III deacetylase that was found to increase lifespan in yeast.[2] Its mammalian orthologue SIRT1 senses caloric restriction, improves insulin secretion in pancreatic beta

* Corresponding author. Tel: +41 44 635 6467, Fax: +41 44 635 6827, Email: christian.matter@access.uzh.ch

cells, and reduces accumulation of fatty acids in white adipose tissue (WAT).[3–5] Various targets of SIRT1 have been characterized, including PPARγ coactivator 1α (PGC-1α), nuclear factor κB (NF-κB), p53, FOXO transcription factors, and endothelial nitric oxide synthase (eNOS).[6–13] Interestingly, many of these targets that are critically involved in regulating metabolism have also been shown to play a role in atherogenesis.[14–18] However, little is known about the relevance of SIRT1 in the latter.

In atherogenesis, chronic endothelial dysfunction is a trigger of plaque formation,[19] and endothelial *SIRT1* overexpression has been shown to prevent atherosclerosis by improving vascular function.[20] Nevertheless, the relevance of SIRT1 on the cellular and molecular events governing atherogenesis is unknown. As multiple targets of SIRT1 may play a role in plaque formation, it is likely that eNOS is not the only mechanism by which SIRT1 prevents atherogenesis. In particular, the role of SIRT1 in monocyte adhesion, macrophage infiltration, lipid uptake, and foam cell formation remains to be determined.

To investigate the role of SIRT1 in these cellular and molecular processes, we compared hypercholesterolaemic *ApoE*$^{-/-}$ *SIRT1*$^{+/+}$ with *ApoE*$^{-/-}$ *SIRT1*$^{+/-}$ mice. These mice have an *SIRT1* haploinsufficiency, but do not display the autoimmune and dysmorphic phenotype of *SIRT1*$^{-/-}$ mice.[21,22]

Methods

Animals

SIRT1 knockout mice on a 129 background[22] were crossed into *ApoE*$^{-/-}$ C57BL/6 mice[23] to generate *ApoE*$^{-/-}$ *SIRT1*$^{+/-}$ mice and *ApoE*$^{-/-}$ *SIRT1*$^{+/+}$ littermates. Of those, male mice were fed a high-cholesterol diet (1.25% total cholesterol, Research Diets) for 12 weeks starting at the age of 8 weeks. Because the few *ApoE*$^{-/-}$ *SIRT1*$^{-/-}$ mice showed a similar dysmorphic phenotype as *SIRT1*$^{-/-}$ mice,[21,22] we did not use them in this study. All animal procedures were approved by the local animal committee and performed in accordance with our institutional guidelines.

Bone marrow transplantation

Bone marrow donor mice were *ApoE*$^{-/-}$ *SIRT1*$^{+/-}$ ($n = 3$; pooled) and *ApoE*$^{-/-}$ *SIRT1*$^{+/+}$ ($n = 3$; pooled) mice, and recipients pure *ApoE*$^{-/-}$ mice (from Jackson Laboratories). Donor mice were split—dose-irradiated under SPF conditions in filter cages with a total irradiation of 1100 rad.[24] Recipient mice were injected intravenously with 10^6 bone marrow cells (*ApoE*$^{-/-}$ *SIRT1*$^{+/-}$ → 7 *ApoE*$^{-/-}$ mice; *ApoE*$^{-/-}$ *SIRT1*$^{+/+}$ → 6 *ApoE*$^{-/-}$ mice). Transplanted mice recovered for 5 weeks and were then fed a high-cholesterol diet for 11 weeks.

Lipoprotein uptake

RAW 264.7 and thioglycolate-elicited peritoneal macrophages were starved for 48 h and then incubated with 10 μg/mL oxLDL for 2 h at 37°C/5% CO_2. After washing away unspecifically bound LDL, cells were fixed and stained with Oil red O (ORO). Experiments were done twice with six independent pools isolated from six mice of each genotype, ORO staining analysed using a light microscope and quantified using analySIS. Low-density lipoprotein uptake was quantified as the ratio of the percentage of the ORO-positive area divided by the percentage of the total cell area in at least 150 cells per genotype. For CD36 blocking studies, RAW 264.7 macrophages were first pre-stimulated for 5 h with 10 ng/mL murine TNFα, and then pre-incubated with 2 μg/mL mouse anti-CD36 (Cascade Bioscience) before adding 10 μg/mL oxLDL over night.

Cell culture

Murine RAW 264.7 cells (Mouse leukaemic monocyte macrophage cell line) were treated with 200 μM splitomicin (Sigma-Aldrich) to perform cholesterol efflux and oxLDL uptake studies. RAW 264.7 cells were stimulated for with 10 ng/mL murine TNFα for 5 h. *SIRT1*$^{-/-}$ mouse embryonic fibroblasts (MEF)[25] were kindly provided by Frederick W. Alt (Harvard University, Boston, MA, USA), and *RelA/p65*$^{-/-}$ MEF with reconstituted wt-RelA/p65 or non-acetylatable RelA/p65 were described previously.[26]

Plasmid and siRNA transfection

Transient transfection of pcDNA3.1::SIRT1 or siRNA into RAW 264.7 or MEF were done with lipofectamin 2000 or lipofectamin RNAi MAX (both Invitrogen). The oligos used for SIRT1-siRNA have been described previously.[5]

Immunohistochemistry and immunocytochemistry

Serial cryosections from the aortic sinus were stained with ORO, rat anti-CD68, rat anti-CD3 (Abcam), rat anti-CD31, rabbit anti-SIRT1 (Upstate/Millipore). Means were taken from $n = 6$ different mice evaluating six serial cryosections/tissue from each mouse. Thoraco-abdominal aortae were fixed and plaques stained with ORO. Collagen, fibrous cap thickness, and necrotic core size were analysed by Elastica van Gieson and Massons trichrome stainings. Cell death was assessed with the terminal deoxyribonucleotidyl transferase-mediated dUTP nick-end labelling kit (Roche).

RNA and protein analysis

Total RNA isolated from proximal aortae was extracted with TRIZOL (Invitrogen), reverse transcribed, and the cDNA quantified by SYBR green qPCR using specific primers. For protein analysis, aortic tissue lysates were blotted and incubated with rabbit anti-SIRT1 (Upstate/Millipore), rabbit anti-eNOS, rabbit anti-phospho-eNOS (Ser1177).

Cholesterol efflux

For cholesterol efflux experiments, RAW 264.7 cells were labelled with 2 μCi/mL [1,2-^{3}H]cholesterol (Perkin Elmer) for 24 h. Following the labelling period, cells were washed and allowed to equilibrate overnight in DMEM containing 0.2% BSA supplemented with cholesterol in the presence or absence of 0.1 mM splitomicin together with 0.3 mM 8-Br-cAMP or 22(R)-HC and 9-cisRA (Sigma). After 24 h stimulation, cells were washed and incubated for 6 h in DMEM containing 0.2% BSA in the presence or absence of 28 μg/mL lipid-free apoA-I. The radioactivity recovered in the culture medium and cell lysates was measured. The apoA-I-mediated cholesterol efflux was calculated as the percentage of total [1,2-^{3}H]cholesterol released into the medium after subtracting the values obtained in the absence of apoA-I. The cholesterol efflux assays were performed in duplicates with three pairs per treatment group.

Plasma lipids and cytokines

Total plasma cholesterol, triglycerides, and free fatty acids were analysed using TR13421, TR22421 (Thermo Electron, Inc.), and 994–75409 (Wako Chemicals). The lipid distribution in plasma lipoprotein fractions was assessed by fast-performance liquid chromatography gel filtration with a Superose 6 HR 10/30 column (Pharmacia).[27] Plasma values of VCAM-1 (MVC00) and ICAM-1 (MIC100; R&D) were

determined using ELISA, and TGF-β, IFNγ, IL-6, IL-10, and mKC using multiplex array systems (Becton, Dickinson and Company).

Flow cytometry

For blood and spleen FACS analyses, single cell suspensions were incubated with antibodies against CD4, CD8, B220, CD11c, CD11b, CD62L, CD44, and CD25 (BD Pharmingen) and then cells were analysed with a FACSCantoII (BD Pharmingen) and FACSDiva software. Post-acquisition analysis was done with FACSDiva (BD Pharmingen) or FlowJo7 software (Tree Star).

Statistical analysis

Data are presented as mean ± SEM. The en face ORO quantifications were analysed with a non-parametric Mann–Whitney *U*-test. Statistical significance of differences was calculated using an ANOVA with *post hoc* Tukey's test or Student unpaired *t*-test. Significance was accepted at the level of $P < 0.05$.

Results

SIRT1 protects against atherosclerosis

To address the role of SIRT1 in atherogenesis, we compared SIRT1 expression in aortic lysates obtained from atherosclerotic *ApoE*$^{-/-}$ and normal wild-type (WT) mice. Aortic SIRT1 protein expression was lower in *ApoE*$^{-/-}$ than in WT mice (see Supplementary material online, *Figure S1A*), suggesting a protective role of SIRT1 in atherogenesis. In order to establish a cause–effect relationship between SIRT1 expression and atherosclerosis, we applied genetic deletion of *SIRT1* in atherosclerotic mice. For this purpose, we compared 20-week-old male *ApoE*$^{-/-}$ *SIRT1*$^{+/+}$ and *ApoE*$^{-/-}$ *SIRT1*$^{+/-}$ mice that were kept on a high-cholesterol diet for 12 weeks (see Supplementary material online, *Figure S2A*). Of note, SIRT1 expression is only slightly reduced in WT mice treated with a high-cholesterol diet (see

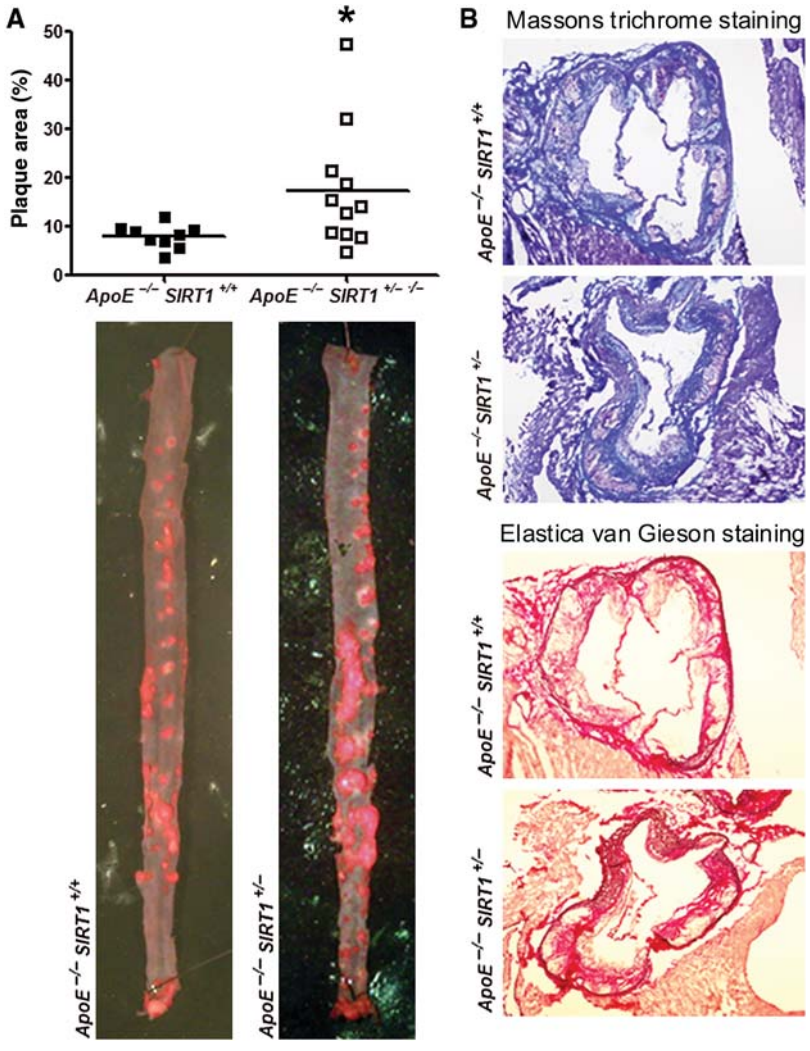

Figure 1 SIRT1 protects mice against atherosclerosis. (*A*) *En face* Oil red O (ORO) staining of thoraco-abdominal aortae and quantifications of plaque area. $n = 9$, *ApoE*$^{-/-}$ *SIRT1*$^{+/+}$(■); $n = 11$, *ApoE*$^{-/-}$ *SIRT1*$^{+/-}$(□). (*B*) Representative images for Massons trichrome and Elastica van Gieson stainings from animals with comparable plaque sizes. Magnification: X 40. *$P < 0.05$.

Supplementary material online, *Figure S1B*). To examine any SIRT1 compensation for the missing *SIRT1* allele, we assessed SIRT1 expression in aortic lysates of the two genotypes. Aortic SIRT1 protein in *ApoE*$^{-/-}$ *SIRT1*$^{+/-}$ mice amounted to about 60% of protein in *ApoE*$^{-/-}$ *SIRT1*$^{+/+}$ mice (see Supplementary material online, *Figure S1C*). Importantly, *en face* plaque quantifications in thoraco-abdominal aortae and in serial cross sections of aortic roots revealed fewer atherosclerotic plaques in *ApoE*$^{-/-}$ *SIRT1*$^{+/+}$ compared with *ApoE*$^{-/-}$ *SIRT1*$^{+/-}$ mice (*Figures 1A* and *2*). Massons trichrome and van Gieson stainings revealed that total collagen content, necrotic core size, and fibrous cap thickness did not differ between the two groups (*Figure 1B*, see Supplementary material online, *Figure S1D–F*). No difference was observed in the amount of apoptotic cells (see Supplementary material online, *Figure S1F*). These findings indicate that endogeneous SIRT1 protects against atherosclerosis.

Accumulation of plaque macrophages and T cells is reduced by SIRT1

Accumulation of macrophages and T cells in the subintimal space plays a central role in atherogenesis.[1] Our analyses revealed increased accumulation of macrophages and T cells in atherosclerotic plaques of *ApoE*$^{-/-}$ *SIRT1*$^{+/-}$ compared with *ApoE*$^{-/-}$ *SIRT1*$^{+/+}$ mice (*Figure 2*). SIRT1 staining in aortae of healthy WT mice or *ApoE*$^{-/-}$ mice under normal diet showed that SIRT1 is expressed in smooth muscle and endothelial cells (see Supplementary material online, *Figure S3A*). In diseased aortae from *ApoE*$^{-/-}$ mice under high-cholesterol diet, SIRT1 is also expressed in cells within the plaques (see Supplementary material online, *Figure S3A*). Double stainings revealed that SIRT1 is expressed in both plaque endothelial cells and macrophages in diseased *ApoE*$^{-/-}$ aortae (see Supplementary material online, *Figure S3B*).

SIRT1 in macrophages is sufficient to reduce foam cell formation and atherogenesis

We observed no difference neither in fasted nor fed plasma glucose or insulin levels, total body or epididymal fat weight (see Supplementary material online, *Figure S4*) and found no difference in total cholesterol and its subfractions between *ApoE*$^{-/-}$ *SIRT1*$^{+/+}$ and *ApoE*$^{-/-}$ *SIRT1*$^{+/-}$ mice (see Supplementary material online, *Figure S5* and *Table S1*). Further, plasma cytokine levels were similar in the two genotypes (see Supplementary material online, *Table S2*). Since inflammatory factors from WAT may enhance atherogenesis,[28,29] we examined the expression of several adipokines and adipose-derived hormones in epididymal WAT. Expression of *Adiponectin* (*Adipoq*), *Leptin*, *Visfatin* (*Nampt*), *Chemerin* (*Rarres2*), *Resistin* (*Retn*) were equivalent, whereas expression of *Plasminogen activator inhibitor 1* (*PAI-1* or *Serpine1*) was slightly, but not significantly elevated in *ApoE*$^{-/-}$ *SIRT1*$^{+/-}$ compared with *ApoE*$^{-/-}$ *SIRT1*$^{+/+}$ epididymal WAT (see

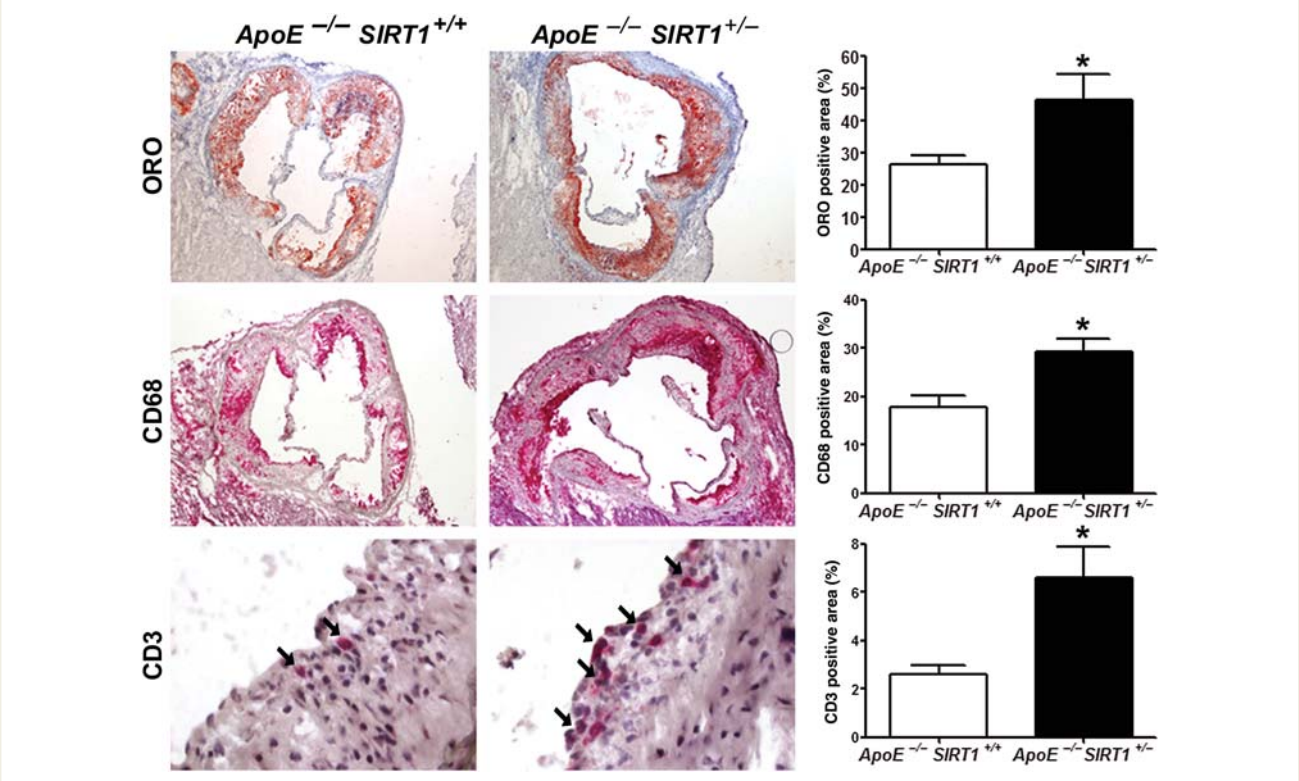

Figure 2 *SIRT1* deletion increases macrophage and T-cell accumulation in plaques. Immunohistochemistry with quantifications of Oil red O (ORO), CD68, and CD3 (arrows) on plaques from aortic sinus. Magnifications: Oil red O, CD68: ×40; CD3: ×400. $n = 6$ per genotype. *$P < 0.05$.

Supplementary material online, *Figure S6*). These data do not exclude a contribution of systemic inflammatory factors such as WAT, but suggest that the damaging effects of partial *SIRT1* deficiency are mainly mediated via inflammatory cells localized in plaques.

Therefore, we focused on the role of SIRT1 in macrophages. Foam cell formation is a crucial step in atherogenesis.[1] We observed no difference in basal LDL uptake in peritoneal-elicited macrophages from $ApoE^{-/-}$ $SIRT1^{+/-}$ compared with $ApoE^{-/-}$ $SIRT1^{+/+}$ mice, but found enhanced uptake upon stimulation with oxLDL (*Figure 3A*). Pharmacological inhibition of SIRT1 with splitomicin in RAW 264.7 macrophages showed a trend towards increasing oxLDL uptake (see Supplementary material online, *Figure S7*). Consistently, siRNA-induced SIRT1 knockdown increased uptake of oxLDL in RAW 264.7 macrophages compared with control cells (*Figure 3B* and *C*). To study a potential role of CD36 in oxLDL uptake, we blocked CD36-mediated oxLDL uptake using an anti-CD36 antibody in scrambled or SIRT1-siRNA-treated macrophages. Neutralization of CD36 decreased uptake of oxLDL by ~50% compared with non-neutralized cells (*Figure 3C*). A higher elevation of oxLDL uptake was observed in SIRT1-siRNA-treated macrophages with additional CD36 neutralization, but did not reach significance difference compared with any other group (*Figure 3C*). These

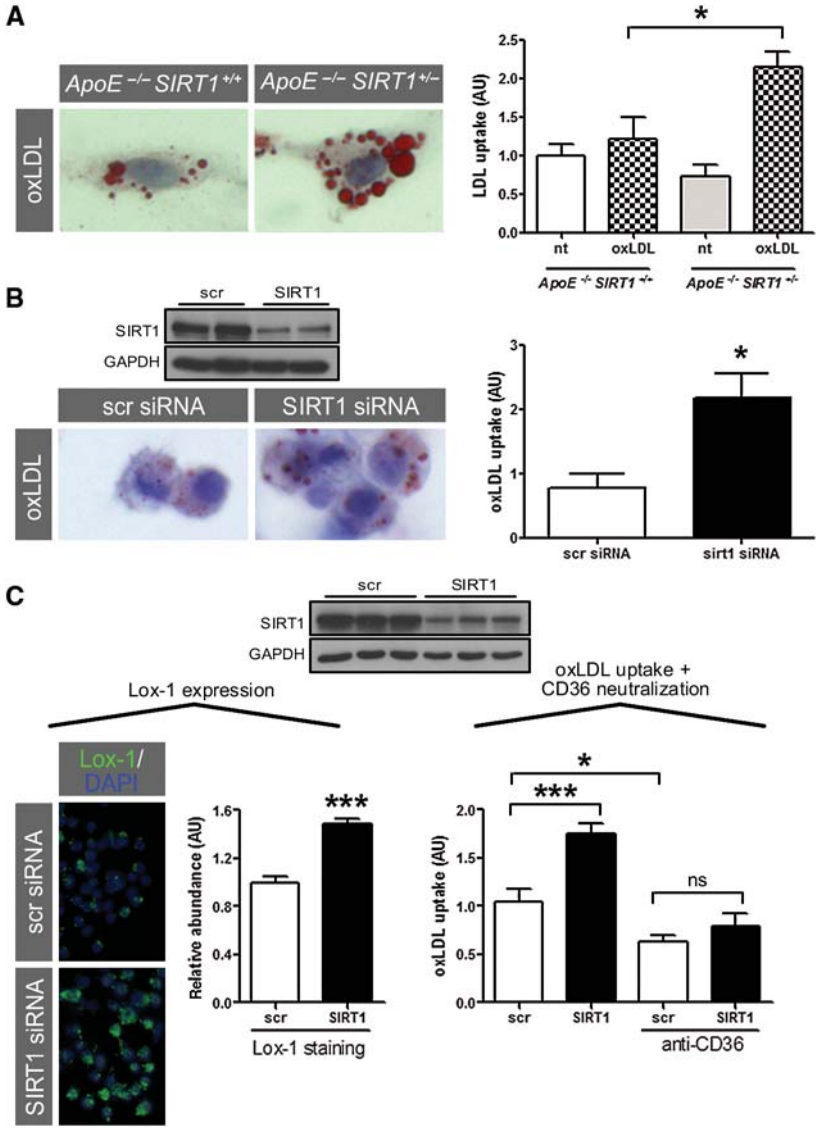

Figure 3 SIRT1 reduces foam cell formation. (*A*) Increased uptake of oxLDL in peritoneal thioglycolate-elicited macrophages from $ApoE^{-/-}$ $SIRT1^{+/-}$ compared with $ApoE^{-/-}$ $SIRT1^{+/+}$ mice. oxLDL uptake is given as the ratio of the percentage of ORO-positive area divided by the percentage of total cell area in at least 150 cells per genotype. (*B*) siRNA-induced SIRT1 knockdown increases uptake of oxLDL in RAW 264.7 macrophages compared with scr-siRNA-treated cells. (*C*) siRNA-mediated SIRT1 silencing in 5 h TNFα-pretreated RAW 264.7 macrophages: left panel, expression of Lox-1; right panel, uptake of oxLDL in neutralizing anti-CD36 antibody-treated cells. $*P < 0.05$. $***P < 0.001$. Magnifications: ×400.

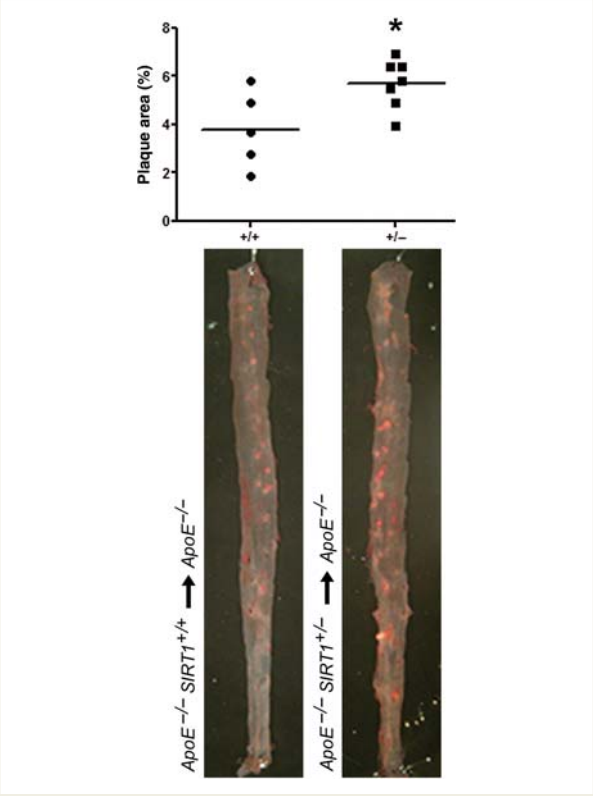

Figure 4 SIRT1 function in macrophages is sufficient to decrease atherogenesis. Chimeric *ApoE*$^{-/-}$ mice that received *ApoE*$^{-/-}$ *SIRT1*$^{+/-}$ ($n = 7$) bone marrow cells develop more atherosclerosis than those which received *ApoE*$^{-/-}$ *SIRT1*$^{+/+}$ ($n = 5$) bone marrow cells. *$P < 0.05$.

data suggest that SIRT1 exerts CD36-dependent and -independent effects in oxLDL uptake.

To examine whether an SIRT1-dependent mechanism in macrophages accounts for decreased atherosclerosis *in vivo*, we performed bone marrow transplantation experiments. Bone marrow from *ApoE*$^{-/-}$ *SIRT1*$^{+/-}$ or *ApoE*$^{-/-}$ *SIRT1*$^{+/+}$ mice was transplanted into irradiated 6-week-old *ApoE*$^{-/-}$ mice (see Supplementary material online, *Figure S2B*), respectively. Flow cytometry analyses of blood and spleen samples from transplanted mice revealed an increased number of blood monocytes of *ApoE*$^{-/-}$ recipient mice receiving *ApoE*$^{-/-}$ *SIRT1*$^{+/-}$ bone marrow cells, but no proportional difference in T-cell subtypes, MHCII^{+} cells, B cells or macrophages (see Supplementary material online, *Figure S8*). Chimeric *ApoE*$^{-/-}$ recipient mice receiving *ApoE*$^{-/-}$ *SIRT1*$^{+/-}$ bone marrow showed more atherosclerotic lesions compared with mice transplanted with *ApoE*$^{-/-}$ *SIRT1*$^{+/+}$ bone marrow (*Figure 4*). These findings support the notion that SIRT1 function in macrophages is sufficient to decrease atherogenesis.

Deacetylation of RelA/p65 by SIRT1 diminishes Lox-1 expression

Active uptake of modified cholesterol in macrophages is mainly regulated by SR-A, SR-B, CD36, and Lox-1,[30] whereas cholesterol efflux is driven by ATP-binding cassette transporters.[31] Expression of CD36, SR-A, and SR-B was not altered (see Supplementary material online, *Figure S9*), whereas *Lox-1* expression was higher in *ApoE*$^{-/-}$ *SIRT1*$^{+/-}$ aortic lysates (*Figure 5A*). Because expression of Lox-1 in SIRT1-siRNA-treated macrophages was increased (*Figure 3C*), we planned to study the SIRT1–Lox-1 pathway more in detail. Deletion of *Lox-1* has been shown to reduce atherosclerosis in mice.[32] Since *Lox-1* is an NF-κB target[33] and SIRT1 deacetylates RelA/p65 in murine macrophages,[34] we compared *Lox-1* RNA levels in TNFα-stimulated RAW 264.7 cells pretreated with splitomicin. We observed an increase in *Lox-1* expression in splitomicin-treated macrophages compared with untreated control cells (*Figure 5B*). These data suggest that SIRT1 suppresses NF-κB signalling in macrophages, thereby reducing *Lox-1* expression and oxLDL uptake.

To get more insight into the molecular events underlying SIRT1-dependent NF-κB deacetylation in murine cells, we analysed SIRT1 expression in different MEF cell lines. Ectopic expression of SIRT1 in *SIRT1*$^{-/-}$ MEF reduced *Lox-1* expression upon TNFα treatment (*Figure 5C*). In *RelA/p65*$^{-/-}$ MEF with reconstituted wt-RelA/p65 expression,[26] siRNA-induced SIRT1 knockdown enhanced *Lox-1* expression upon TNFα stimulation. In contrast, SIRT1-siRNA had no effect on *Lox-1* expression in TNFα-stimulated *RelA/p65*$^{-/-}$ MEF with reconstituted non-acetylatable K310R-mutant-RelA/p65[26] (*Figure 5D*). These data show that SIRT1-dependent deacetylation of RelA/p65 at K310 is sufficient to reduce *Lox-1* gene expression.

Several reports show a link between Lox-1 and matrix metalloproteinases (MMPs) that are expressed and secreted by human endothelial cells, including the collagenase MMP1, stromelysin-1 (MMP3), the membrane type 1 MMP (MT1-MMP or MMP14), and the tissue inhibitor of metalloproteinase 3 (TIMP3).[35–38] To investigate if metalloproteinase expression is affected by SIRT1, we quantified aortic expression of *MMP13*, *MMP3*, *MMP8*, *MMP9*, *MMP14*, and *TIMP3*. No significant change in the expression of these MMPs was observed in *ApoE*$^{-/-}$ *SIRT1*$^{+/-}$ compared with *ApoE*$^{-/-}$ *SIRT1*$^{+/+}$ aortae (see Supplementary material online, *Figure S10*), indicating that the phenotype of *ApoE*$^{-/-}$ *SIRT1*$^{+/-}$ mice is not related to SIRT1–Lox-1-mediated expression of MMPs.

Atheroprotective effects of SIRT1 do not affect cholesterol efflux

When examining cholesterol efflux, we found that expression of *ABCA1* was not altered in aortic lysates from *ApoE*$^{-/-}$ *SIRT1*$^{+/-}$ compared with *ApoE*$^{-/-}$ *SIRT1*$^{+/+}$ mice (see Supplementary material online, *Figure S11A*). Similarly, expression levels of *ABCA1* and *ABCG1* were not different in peritoneal macrophages from *ApoE*$^{-/-}$ *SIRT1*$^{+/+}$ and *ApoE*$^{-/-}$ *SIRT1*$^{+/-}$ mice (see Supplementary material online, *Figure S11B*). Cholesterol efflux assays in RAW 264.7 macrophages treated with splitomicin revealed no ApoA-I-dependent changes (see Supplementary material online, *Figure S11C*). Furthermore, we detected no difference in aortic expression of the ABCA1 regulators LXRα, PPARγ, or its coactivator PGC-1α (PPARγ coactivator 1α) (see Supplementary material online, *Figure S11D–F*). These data suggest that aortic cholesterol efflux is not affected by SIRT1 in atherosclerotic mice.

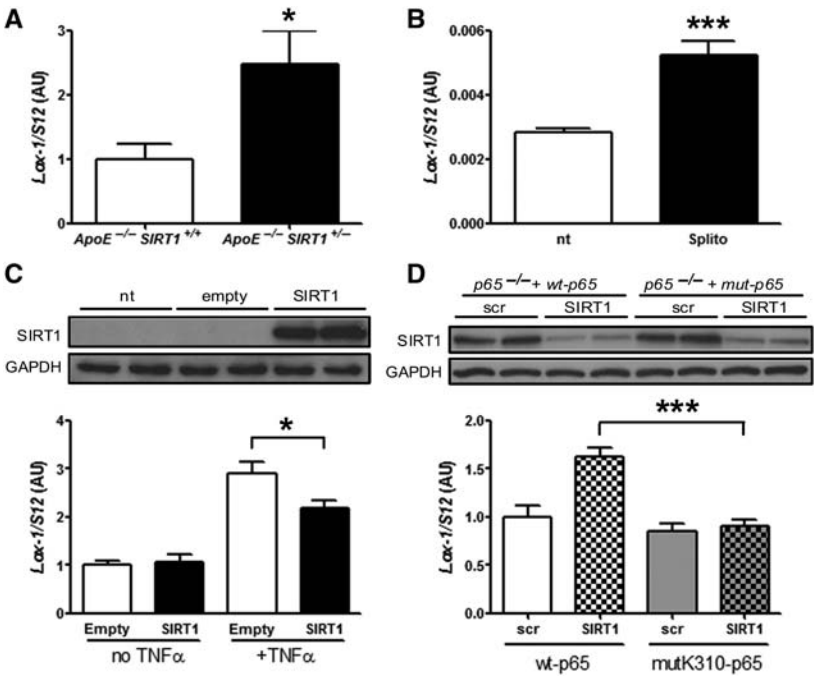

Figure 5 Deacetylation of RelA/p65 by SIRT1 diminishes Lox-1 expression. (*A*) Aortic *Lox-1* expression is increased in $ApoE^{-/-}$ $SIRT1^{+/-}$ compared with $ApoE^{-/-}$ $SIRT1^{+/+}$ mice. (*B*) *Lox-1* expression is higher in 5 h TNFα-stimulated RAW 264.7 macrophages pretreated with 200 μM splitomicin (Splito) compared with untreated cells (nt). (*C*) Ectopic *SIRT1* expression in $SIRT1^{-/-}$ MEF reduces *Lox-1* expression. (*D*) In *RelA/p65*$^{-/-}$ MEF with reconstituted wt-RelA/p65, siRNA-mediated SIRT1 knockdown enhances *Lox-1* expression upon 5 h TNFα stimulation, whereas no effect is observed in *RelA/p65*$^{-/-}$ MEF with a reconstituted mutated, non-acetylatable K310-RelA/p65. *$P < 0.05$; ***$P < 0.001$.

Discussion

Recently, SIRT1 has been shown to decrease atherosclerosis by improving endothelium-dependent vascular function in $ApoE^{-/-}$ mice with an endothelial SIRT1 overexpression that were kept on a high-fat diet.[20] Our study shows that endogenous SIRT1 prevents macrophage foam cell formation in atherogenesis independently of systemic lipid levels. We demonstrate that loss of a single *SIRT1* allele in $ApoE^{-/-}$ $SIRT1^{+/-}$ mice is sufficient to increase plaque formation.

Macrophage-derived foam cell formation is enhanced upon a relative increase in cholesterol uptake or by a defective cholesterol efflux, respectively.[39] Our *in vitro* foam cell assay reveals that SIRT1 activation diminishes oxLDL uptake in peritoneal macrophages. Among the receptors that may account for this increased LDL uptake by macrophages, we identified Lox-1 to be critically involved: SIRT1 inhibits TNFα-induced expression of *Lox-1* in macrophages. In fact, the *Lox-1* promoter contains NF-κB binding sites and is expressed upon TNFα stimulation.[33] Using *RelA/p65*$^{-/-}$ MEF, we could further show that the deacetylation of RelA/p65 by SIRT1 suppresses *Lox-1* expression. We acknowledge that the final proof of a Lox-1-mediated effect on foam cell formation would require additional evidence from genetic loss-of-function or neutralizing antibody experiments. These questions need to be addressed in future studies.

To test whether an SIRT1-dependent mechanism in bone marrow-derived cells accounts for the increase in atherosclerosis *in vivo*, we performed bone marrow transplantation experiments. Chimeric $ApoE^{-/-}$ mice receiving $ApoE^{-/-}$ $SIRT1^{+/-}$ bone marrow showed increased atherosclerotic plaques compared with mice receiving $ApoE^{-/-}$ $SIRT1^{+/+}$ bone marrow. These findings demonstrate that partial *SIRT1* deletion in bone marrow-derived macrophages is sufficient to enhance atherogenesis.

The role of NF-κB in plaque macrophages and lipoprotein uptake in atherogenesis is controversial. Disruption of NF-κB signalling by partial *IKK2* deletion in macrophages increased atherosclerosis.[40] Conversely, studies using macrophage-specific *p50* deletion or a dominant-negative *IκBα* mutant to disrupt NF-κB signalling, resulted in smaller atherosclerotic lesions and diminished uptake of lipoproteins.[41,42] Since NF-κB and its transcriptional activity are tightly regulated,[43,44] pharmacological modulation of an upstream regulator of NF-κB seems more promising in preventing atherogenesis than direct NF-κB modulation.[45] Our study shows that SIRT1 might be an attractive modulator, since its interference with the NF-κB signalling pathway exerts beneficial effects on plaque formation.

Several reports suggest that other SIRT1 targets may also contribute to atherogenesis. For instance, PPARγ, a key transcription factor in adipocyte differentiation, plays a pivotal role in macrophages and modulates the extent of atherosclerosis.[14] Both PPARγ and its target LXR are regulated by SIRT1 in adipocytes and macrophages.[5,46] Interestingly, Li *et al.*[46] showed reduced cholesterol efflux in primary macrophages from $SIRT1^{-/-}$ compared with $SIRT1^{+/+}$ mice. We could neither observe a difference

in the aortic expression of ABCA1, ABCG1, PPARγ, or LXRα nor an ApoA-I-dependent decrease in cholesterol efflux upon splitomicin treatment in RAW 264.7 macrophages. Possibly, the effect of a single missing *SIRT1* allele is not sufficient to affect cholesterol efflux in atherosclerotic mice.

Taken together, our results reveal a novel mechanism by which SIRT1 prevents atherogenesis: SIRT1 suppresses NF-signalling by deacetylating RelA/p65, thereby reducing *Lox-1* expression and diminishing uptake of oxLDL and foam cell formation. Given the availability of specific SIRT1-activating drugs that are being tested in clinical trials in patients with type 2 diabetes, pharmacological activation of SIRT1 may also become an attractive anti-atherogenic strategy by preventing macrophage foam cell formation.[47]

Supplementary material

Supplementary material is available at *European Heart Journal* online.

Acknowledgements

We thank Elin Stenfeldt (University of Gothenburg), Sabine Rütti, and Chad E. Brokopp (University Hospital Zurich) for technical assistance and the Center for Microscopy and Image Analysis at the University of Zurich for using their facilities.

Funding

This work was funded by grants from the Swiss National Science Foundation [grant numbers 31-114094/1 to C.M.M. and 3100-068118 to T.F.L.] and the University Research Priority Program 'Integrative Human Physiology' at the University of Zurich. Further support was provided by unrestricted grants from the MERCATOR Foundation Switzerland and a strategic alliance with Pfizer, Inc., New York. Funding to pay the Open Access publication charges for this article was provided by the Swiss National Science Foundation.

Conflict of interest: none declared.

References

1. Libby P. Inflammation in atherosclerosis. *Nature* 2002;**420**:868–874.
2. Kaeberlein M, McVey M, Guarente L. The SIR2/3/4 complex and SIR2 alone promote longevity in *Saccharomyces cerevisiae* by two different mechanisms. *Genes Dev* 1999;**13**:2570–2580.
3. Chen D, Steele AD, Lindquist S, Guarente L. Increase in activity during calorie restriction requires Sirt1. *Science* 2005;**310**:1641.
4. Bordone L, Motta MC, Picard F, Robinson A, Jhala US, Apfeld J, McDonagh T, Lemieux M, McBurney M, Szilvasi A, Easlon EJ, Lin SJ, Guarente L. Sirt1 regulates insulin secretion by repressing UCP2 in pancreatic beta cells. *PLoS Biol* 2006;**4**:e31.
5. Picard F, Kurtev M, Chung N, Topark-Ngarm A, Senawong T, Machado De Oliveira R, Leid M, McBurney MW, Guarente L. Sirt1 promotes fat mobilization in white adipocytes by repressing PPAR-gamma. *Nature* 2004;**429**:771–776.
6. Vaziri H, Dessain SK, Ng Eaton E, Imai SI, Frye RA, Pandita TK, Guarente L, Weinberg RA. hSIR2(SIRT1) functions as an NAD-dependent p53 deacetylase. *Cell* 2001;**107**:149–159.
7. Brunet A, Sweeney LB, Sturgill JF, Chua KF, Greer PL, Lin Y, Tran H, Ross SE, Mostoslavsky R, Cohen HY, Hu LS, Cheng HL, Jedrychowski MP, Gygi SP, Sinclair DA, Alt FW, Greenberg ME. Stress-dependent regulation of FOXO transcription factors by the SIRT1 deacetylase. *Science* 2004;**303**:2011–2015.
8. Motta MC, Divecha N, Lemieux M, Kamel C, Chen D, Gu W, Bultsma Y, McBurney M, Guarente L. Mammalian SIRT1 represses forkhead transcription factors. *Cell* 2004;**116**:551–563.
9. Mattagajasingh I, Kim CS, Naqvi A, Yamamori T, Hoffman TA, Jung SB, DeRicco J, Kasuno K, Irani K. SIRT1 promotes endothelium-dependent vascular relaxation by activating endothelial nitric oxide synthase. *Proc Natl Acad Sci USA* 2007;**104**:14855–14860.
10. Lagouge M, Argmann C, Gerhart-Hines Z, Meziane H, Lerin C, Daussin F, Messadeq N, Milne J, Lambert P, Elliott P, Geny B, Laakso M, Puigserver P, Auwerx J. Resveratrol improves mitochondrial function and protects against metabolic disease by activating SIRT1 and PGC-1alpha. *Cell* 2006;**127**:1109–1122.
11. Rodgers JT, Lerin C, Haas W, Gygi SP, Spiegelman BM, Puigserver P. Nutrient control of glucose homeostasis through a complex of PGC-1alpha and SIRT1. *Nature* 2005;**434**:113–118.
12. Yeung F, Hoberg JE, Ramsey CS, Keller MD, Jones DR, Frye RA, Mayo MW. Modulation of NF-kappaB-dependent transcription and cell survival by the SIRT1 deacetylase. *EMBO J* 2004;**23**:2369–2380.
13. Luo J, Nikolaev AY, Imai S, Chen D, Su F, Shiloh A, Guarente L, Gu W. Negative control of p53 by Sir2alpha promotes cell survival under stress. *Cell* 2001;**107**:137–148.
14. Tontonoz P, Spiegelman BM. Fat and beyond: the diverse biology of PPARgamma. *Annu Rev Biochem* 2008;**77**:289–312.
15. Kim HJ, Park KG, Yoo EK, Kim YH, Kim YN, Kim HS, Kim HT, Park JY, Lee KU, Jang WG, Kim JG, Kim BW, Lee IK. Effects of PGC-1alpha on TNF-alpha-induced MCP-1 and VCAM-1 expression and NF-kappaB activation in human aortic smooth muscle and endothelial cells. *Antioxid Redox Signal* 2007;**9**:301–307.
16. Brand K, Page S, Rogler G, Bartsch A, Brandl R, Knuechel R, Page M, Kaltschmidt C, Baeuerle PA, Neumeier D. Activated transcription factor nuclear factor-kappa B is present in the atherosclerotic lesion. *J Clin Invest* 1996;**97**:1715–1722.
17. Knowles JW, Reddick RL, Jennette JC, Shesely EG, Smithies O, Maeda N. Enhanced atherosclerosis and kidney dysfunction in eNOS(−/−)Apoe(−/−) mice are ameliorated by enalapril treatment. *J Clin Invest* 2000;**105**:451–458.
18. Guevara NV, Kim HS, Antonova EI, Chan L. The absence of p53 accelerates atherosclerosis by increasing cell proliferation *in vivo*. *Nat Med* 1999;**5**:335–339.
19. Kawashima S, Yokoyama M. Dysfunction of endothelial nitric oxide synthase and atherosclerosis. *Arterioscler Thromb Vasc Biol* 2004;**24**:998–1005.
20. Zhang QJ, Wang Z, Chen HZ, Zhou S, Zheng W, Liu G, Wei YS, Cai H, Liu DP, Liang CC. Endothelium-specific overexpression of class III deacetylase SIRT1 decreases atherosclerosis in apolipoprotein E-deficient mice. *Cardiovasc Res* 2008;**80**:191–199.
21. Sequeira J, Boily G, Bazinet S, Saliba S, He X, Jardine K, Kennedy C, Staines W, Rousseaux C, Mueller R, McBurney MW. Sirt1-null mice develop an autoimmune-like condition. *Exp Cell Res* 2008;**314**:3069–3074.
22. McBurney MW, Yang X, Jardine K, Hixon M, Boekelheide K, Webb JR, Lansdorp PM, Lemieux M. The mammalian SIR2alpha protein has a role in embryogenesis and gametogenesis. *Mol Cell Biol* 2003;**23**:38–54.
23. Plump AS, Smith JD, Hayek T, Aalto-Setala K, Walsh A, Verstuyft JG, Rubin EM, Breslow JL. Severe hypercholesterolemia and atherosclerosis in apolipoprotein E-deficient mice created by homologous recombination in ES cells. *Cell* 1992;**71**:343–353.
24. Becher B, Durell BG, Miga AV, Hickey WF, Noelle RJ. The clinical course of experimental autoimmune encephalomyelitis and inflammation is controlled by the expression of CD40 within the central nervous system. *J Exp Med* 2001;**193**:967–974.
25. Chua KF, Mostoslavsky R, Lombard DB, Pang WW, Saito S, Franco S, Kaushal D, Cheng HL, Fischer MR, Stokes N, Murphy MM, Appella E, Alt FW. Mammalian SIRT1 limits replicative life span in response to chronic genotoxic stress. *Cell Metab* 2005;**2**:67–76.
26. Buerki C, Rothgiesser KM, Valovka T, Owen HR, Rehrauer H, Fey M, Lane WS, Hottiger MO. Functional relevance of novel p300-mediated lysine 314 and 315 acetylation of RelA/p65. *Nucleic Acids Res* 2008;**36**:1665–1680.
27. Purcell-Huynh DA, Farese RV Jr, Johnson DF, Flynn LM, Pierotti V, Newland DL, Linton MF, Sanan DA, Young SG. Transgenic mice expressing high levels of human apolipoprotein B develop severe atherosclerotic lesions in response to a high-fat diet. *J Clin Invest* 1995;**95**:2246–2257.
28. Trayhurn P, Wood IS. Adipokines: inflammation and the pleiotropic role of white adipose tissue. *Br J Nutr* 2004;**92**:347–355.
29. Lyon CJ, Law RE, Hsueh WA. Minireview: adiposity, inflammation, and atherogenesis. *Endocrinology* 2003;**144**:2195–2200.
30. Moore KJ, Freeman MW. Scavenger receptors in atherosclerosis: beyond lipid uptake. *Arterioscler Thromb Vasc Biol* 2006;**26**:1702–1711.
31. Tiwari RL, Singh V, Barthwal MK. Macrophages: an elusive yet emerging therapeutic target of atherosclerosis. *Med Res Rev* 2008;**28**:483–544.
32. Mehta JL, Sanada N, Hu CP, Chen J, Dandapat A, Sugawara F, Satoh H, Inoue K, Kawase Y, Jishage K, Suzuki H, Takeya M, Schnackenberg L, Beger R, Hermonat PL, Thomas M, Sawamura T. Deletion of LOX-1 reduces atherogenesis in LDLR knockout mice fed high cholesterol diet. *Circ Res* 2007;**100**:1634–1642.
33. Nagase M, Abe J, Takahashi K, Ando J, Hirose S, Fujita T. Genomic organization and regulation of expression of the lectin-like oxidized low-density lipoprotein receptor (LOX-1) gene. *J Biol Chem* 1998;**273**:33702–33707.
34. Shen Z, Ajmo JM, Rogers CQ, Liang X, Le L, Murr MM, Peng Y, You M. Role of SIRT1 in regulation of LPS- or two ethanol metabolites-induced TNF{alpha} production in cultured macrophage cell lines. *Am J Physiol Gastrointest Liver Physiol* 2009;**296**:G1047–1053.

35. Sugimoto K, Ishibashi T, Sawamura T, Inoue N, Kamioka M, Uekita H, Ohkawara H, Sakamoto T, Sakamoto N, Okamoto Y, Takuwa Y, Kakino A, Fujita Y, Tanaka T, Teramoto T, Maruyama Y, Takeishi Y. LOX-1-MT1-MMP axis is crucial for RhoA and Rac1 activation induced by oxidized low-density lipoprotein in endothelial cells. *Cardiovasc Res* 2009;**84**:127–136.
36. Kakinuma T, Yasuda T, Nakagawa T, Hiramitsu T, Akiyoshi M, Akagi M, Sawamura T, Nakamura T. Lectin-like oxidized low-density lipoprotein receptor 1 mediates matrix metalloproteinase 3 synthesis enhanced by oxidized low-density lipoprotein in rheumatoid arthritis cartilage. *Arthritis Rheum* 2004;**50**:3495–3503.
37. Li D, Liu L, Chen H, Sawamura T, Ranganathan S, Mehta JL. LOX-1 mediates oxidized low-density lipoprotein-induced expression of matrix metalloproteinases in human coronary artery endothelial cells. *Circulation* 2003;**107**:612–617.
38. Li D, Williams V, Liu L, Chen H, Sawamura T, Antakli T, Mehta JL. LOX-1 inhibition in myocardial ischemia-reperfusion injury: modulation of MMP-1 and inflammation. *Am J Physiol Heart Circ Physiol* 2002;**283**:H1795–H1801.
39. Li AC, Glass CK. The macrophage foam cell as a target for therapeutic intervention. *Nat Med* 2002;**8**:1235–1242.
40. Kanters E, Pasparakis M, Gijbels MJ, Vergouwe MN, Partouns-Hendriks I, Fijneman RJ, Clausen BE, Forster I, Kockx MM, Rajewsky K, Kraal G, Hofker MH, de Winther MP. Inhibition of NF-kappaB activation in macrophages increases atherosclerosis in LDL receptor-deficient mice. *J Clin Invest* 2003;**112**:1176–1185.
41. Ferreira V, van Dijk KW, Groen AK, Vos RM, van der Kaa J, Gijbels MJ, Havekes LM, Pannekoek H. Macrophage-specific inhibition of NF-kappaB activation reduces foam-cell formation. *Atherosclerosis* 2007;**192**:283–290.
42. Kanters E, Gijbels MJ, van der Made I, Vergouwe MN, Heeringa P, Kraal G, Hofker MH, de Winther MP. Hematopoietic NF-kappaB1 deficiency results in small atherosclerotic lesions with an inflammatory phenotype. *Blood* 2004;**103**:934–940.
43. Cheong R, Hoffmann A, Levchenko A. Understanding NF-kappaB signaling via mathematical modeling. *Mol Syst Biol* 2008;**4**:192.
44. Gilmore TD. Introduction to NF-kappaB: players, pathways, perspectives. *Oncogene* 2006;**25**:6680–6684.
45. Ahn KS, Sethi G, Aggarwal BB. Nuclear factor-kappa B: from clone to clinic. *Curr Mol Med* 2007;**7**:619–637.
46. Li X, Zhang S, Blander G, Tse JG, Krieger M, Guarente L. SIRT1 deacetylates and positively regulates the nuclear receptor LXR. *Mol Cell* 2007;**28**:91–106.
47. Milne JC, Lambert PD, Schenk S, Carney DP, Smith JJ, Gagne DJ, Jin L, Boss O, Perni RB, Vu CB, Bemis JE, Xie R, Disch JS, Ng PY, Nunes JJ, Lynch AV, Yang H, Galonek H, Israelian K, Choy W, Iffland A, Lavu S, Medvedik O, Sinclair DA, Olefsky JM, Jirousek MR, Elliott PJ, Westphal CH. Small molecule activators of SIRT1 as therapeutics for the treatment of type 2 diabetes. *Nature* 2007;**450**:712–716.

CARDIOVASCULAR FLASHLIGHT

doi:10.1093/eurheartj/ehq192
Online publish-ahead-of-print 10 June 2010

Pottery heart

Radoslaw Grabysa*

Clinic of Internal Diseases, Gastroenterology and Hepatology, Warmia and Mazury University, University Hospital, Olsztyn 10-082, Poland

* Corresponding author. Tel: +48 72 8323308, Fax: +48 89 5273624, Email: rgraby@wp.pl

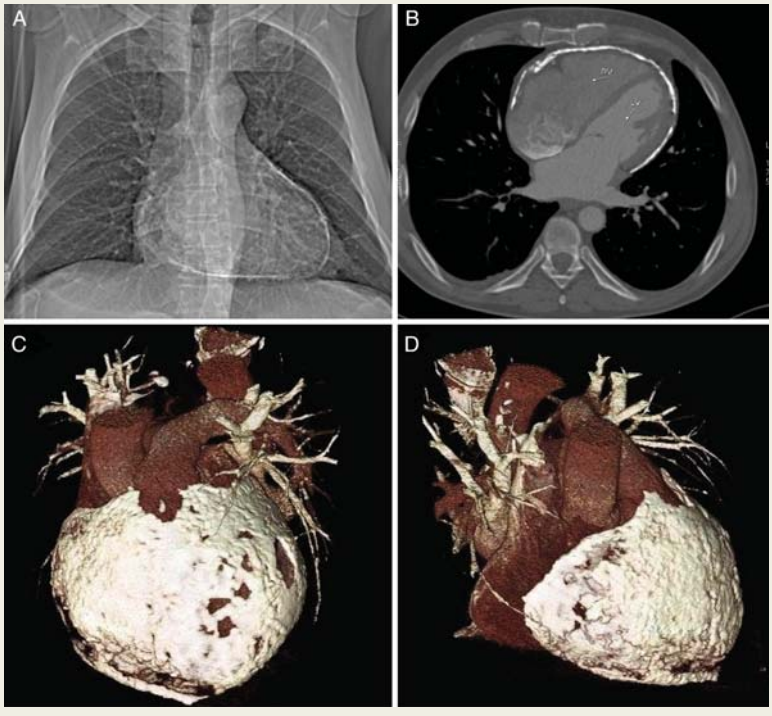

A 52-year-old man presented with arterial hypertension and 1-year history of progressive shortness of breath, fatigue and abdominal swelling. Physical examination revealed hypotension, tachycardia, muffled heart sounds, distension of the jugular veins with Kussmaul's sign and ascites. Blood pressure was 90/75 mmHg and heart rate was 100 b.p.m. Laboratory tests, including inflammatory markers and kidney function were normal. Tuberculosis was also excluded. ECG showed sinus tachycardia with P-mitrale and low QRS voltage. Chest X-ray revealed dense pericardial calcification (*Panel A*). A transthoracic echocardiography was conducted with very poor acoustic window and was positive only for diastolic dysfunction. Multidetector computed cardiac tomography scans of the chest revealed diffuse thickening and calcification involving both the visceral and parietal pericardium of right and left ventricles (RV, LV) (*Panel B*, arrows) and confirmed the diagnosis of constrictive pericarditis. Volume rendering reconstruction of cardiac structures showed dense pericardial calcification predominantly over both the ventricles resembling heart made with porcelain (*Panels C* and *D*). The patient was qualified for surgical pericardiectomy, which resulted in immediate normalization of cardiac function. The calcified pericardium was presumed to be owing to misdiagnosed chronic pericarditis.

Panel A. Chest X ray (postero-anterior view) showing pericardial calcification.

Panel B. Multidetector computed cardiac tomography showing diffuse thickening and calcification of the pericardium (arrows).

Panels C and *D*. Volume rendering reconstruction of cardiac structures showing dense pericardial calcification predominantly over both the ventricles ('pottery heart').